BA, which is responsible to a β3-adrenergic receptor agonist, has also been generated from human multipotent adipose-derived stem cells by chronic treatment with thiazolidinediones (Elabd et al., 2009). The merit of our system is that it does not require preparation of human specimen materials but utilizes hPSCs, which are capable of unlimited expansion in vitro.

One of the main findings of our research is that HC composed of KITLG, IL6, FLT3LG, and VEGF is essential for BA differentiation of hPSCs. Although BMP7 plays an important role in BA differentiation of hPSC (Figure S2) as reported in murine cases (Tseng et al., 2008), HC is indispensable for BA differentiation of hPSCs (Figure 1D). It is known that VEGF is synthesized in rodent BAT (Asano et al., 1997; Tonello et al., 1999), promoting the angiogenesis within BAT. Moreover, IL6 is reportedly secreted from cultured human BM adipocytes (Laharrague et al., 2000). Our findings imply that VEGF and IL6, together with KITLG and FLT3LG, work as fundamental autocrine or paracrine factors to promote BA differentiation.

Compatible to the finding by Sellayah et al. (Sellayah et al., 2011), the inhibitor analyses demonstrated the involvement of p38 MAPK signaling, but not of MEK signaling, in BA differentiation of hESC (Figures 5E–5G). However, distinct findings were obtained from the case of hiPSCs, in which MEK signaling played a role in BA differentiation (Figure 5E–5G). At this moment, the basis for the difference in the effects of identical inhibitors between hESCs and hiPSCs remains elusive. It may be related to the difference in the genetic background of pluripotent stem cell lines, reflecting the individual difference of the "donor" or the difference in the type of pluripotent stem cells or both. Further investigations are required to obtain the whole picture of the molecular basis for BA differentiation of hPSCs.

By providing high-purity human BA and WA materials, we demonstrated the differential effects on metabolic regulation between BA and WA: BA improves while WA deteriorates glucose metabolism. Because those effects were confirmed by a short-term assay without body weight changes and also because the effects of BA and WA on lipid metabolism were similar, the beneficial effect of BA on glucose metabolism is not a secondary consequence of general metabolic improvement. Conventional subcutaneous fat transplantation experiments were not able to distinguish the effect of BA from that of WA, because subcutaneous fat tissues contain both WA and BA. Thus, our system will provide a unique tool for the research of BA in regard to glucose metabolism.

Another surprising finding is the functional link between BA and hematopoiesis. We showed that hPSCdBAs serve as a stroma for MPCs. In contrast to the "niche" for HSCs, which is composed of immature osteoblasts and sinusoidal endothelial cells, the "stroma" for committed HPCs remains a mystery. The only report showing the characteristic of such stroma was a study by Dexter et al. (Dexter et al., 1977), in which BM fat cells with multilocular lipid droplets attached by mitochondria were identified as a stroma for CFU-S. Our results indicating that (1) hPSCdBAs express various hematopoietic cytokines in response to β-adrenergic receptor stimuli, (2) hPSCdBAs promote myelopoiesis of human cord blood $CD34^+$ cells, and (3) β-adrenergic receptor stimuli accelerate the recovery from 5-FU-mediated myelosuppression together show that BM-BAT serves as a stroma for MPCs. Among those, the third finding is particularly important because it illustrates a very feasible way to shorten the period of myelosuppression, the major side effect of intensive chemotherapy for progressive cancers.

The PET-CT results of young healthy volunteers, together with gene expression analyses of human BM specimen and histological examinations of murine vertebral BM samples, strongly suggest the existence of active BAT in vertebral BM in mammals. Because classical BAT is derived from *Myf5*-positive myoblastic cells (Seale et al., 2008) and because *Myf5*-positive cells emerge at the juxtaspinal, prospectively paravertebral, regions within somites (Cossu et al., 1996; Braun and Arnold, 1996), the existence of BA in vertebral BM seems reasonable. Because the major portions of vertebrae are composed of trabecular bones, which are the sites of active hematopoiesis, and the vertebral marrow is the last reserve site for hematopoietic activity in aged individuals (Tanaka and Inoue, 1976), the hematopoietic microenvironment of vertebral BM may bear a unique character. Further investigation will elucidate the whole picture of HPC regulation.

Our system, providing highly functional hiPSCdBA, may open a new avenue to the therapy for obesity. However, we have found that BA differentiation efficiencies substantially differ among hiPSC lines (data not shown), as reported in the case of pancreatic β cell differentiation of hESCs (Osafune et al., 2008). For clinical application, selection of appropriate lines of hiPSCs will be as important as sophisticating the whole differentiation process into good manufacturing practice levels.

EXPERIMENTAL PROCEDURES

Establishment of hiPSCs and Provision of hESCs

SeV-iPS cells were established from human neonatal fibroblast or human umbilical vein endothelial cells by introducing Yamanaka's four factors using CytoTune-iPS ver.1.0 (DNAVEC Corp) (Figure S7). Transgenes were eliminated by a 39þC heat treatment for 5 days. A hESC line (KhES-3) was generously provided by the Institute for Frontier Medical Science, Kyoto University (Suemori et al., 2006).

A Directed Differentiation of hESCs/hiPSCs into Functional BA

hESCs or hiPSCs were cultured in a 6 cm low-attachment culture dish using a serum-free differentiation medium composed of 1:1 ratio of IMDM (I3390, Sigma Chemical Co.) and Ham's F12 (087-08335, WAKO Pure Chemical Industries), 5 mg/ml bovine serum albumin (A802, Sigma Chemical Co.), 1:100 synthetic lipids (GIBCO #11905-031, Life Technologies, Inc.), 450 μM α- monothioglycerol (207-09232, WAKO Pure Chemical Industries), 1:100 insulin-transferrin-selenium (ITS-A, Life Technologies, Inc.), 2 mM Glutamax II (GIBCO #35050-061, Life Technologies, Inc.), 5% protein-free hybridoma mix (PFHMII, GIBCO #12040-077, Life Technologies, Inc.), 50 μg/ml ascorbic acid-2-phosphate (Sigma, A-8960), and the hematopoietic cytokine cocktail I (5 ng/ml IGF-II, 20 ng/ml BMP4, 5 ng/ml VEGFA, 20 ng/ml KITLG, 2.5 ng/ml FLT3LG, 2.5 ng/ml IL-6) for 8 days to form spheres. The

immunostaining using an anti-UCP1 antibody (I) and anti-human HLA-A,B,C antibody (J) at day 7. Arrowheads in (H) indicate microvasculatures. Scale bars, 50 μm.

(K–M) Mice were transplanted with hMSCdWAs alone or together with hESCdBA, and OGTT was performed. Fasting blood glucose levels (K), HOMA-IR (L), and blood glucose values after oral glucose loading (M) are shown. The error bars in (A), (B), (D)–(G), (K), (L), and (M) represent average ± SD.

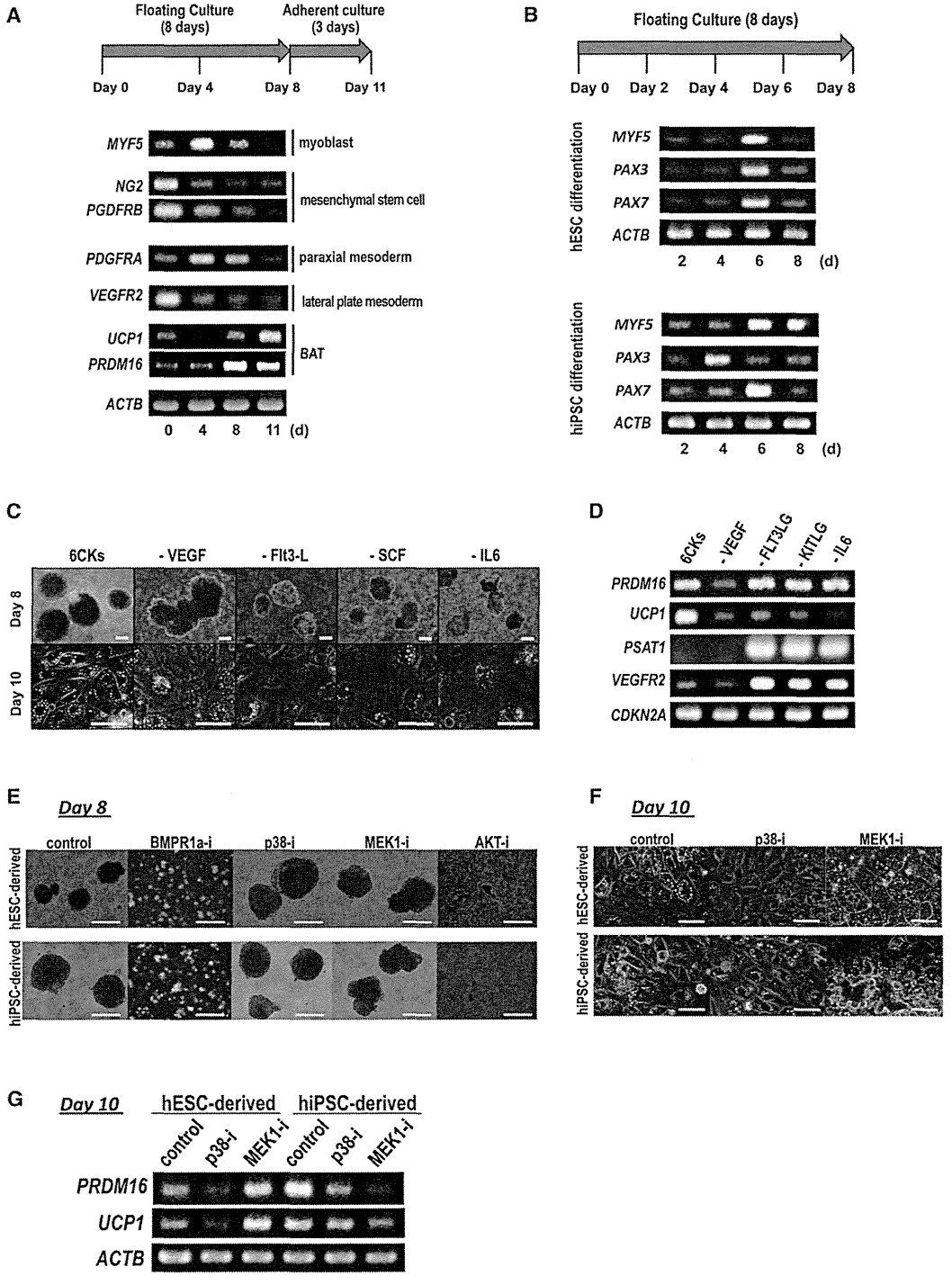

Figure 5. Signals Involved in BA Differentiation

(A) Developmental marker expression was examined by RT-PCR during BA differentiation of hESCs. Similar results were obtained regarding hiPSCs (data not shown).

(B) Myoblastic marker expressions were determined by RT-PCR during floating culture.

(C and D) The role of each cytokine was evaluated by morphological examinations (C) and RT-PCR (D). Scale bar, 100 μm (upper panels); and scale bar, 150 μm (lower panels).

(E–G) Inhibitor analyses. BA differentiation was performed in the presence of inhibitors of BMPR1a, p38 MAPK, MEK1, or AKT as indicated. Phase contrast micrographs of the spheres at day 8 (scale bar, 200 μm) (E) and those of BA at day 10 (scale bar, 50 μm) (F) were shown. Expressions of *UCP1* and *PRDM16* were determined at day 10 by RT-PCR (G).

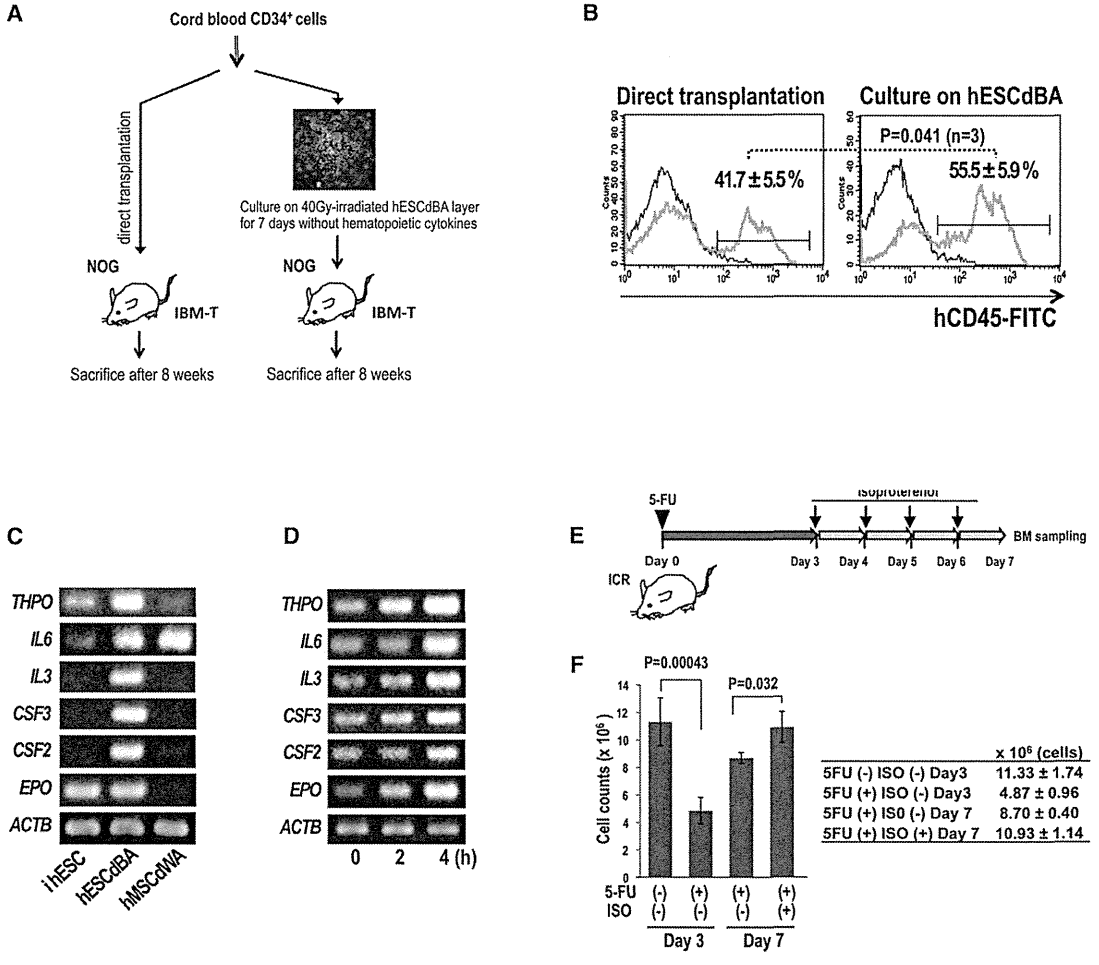

Figure 6. Hematopoietic Stromal Assays

(A) Schematic presentation of the assay.

(B) After 8 weeks from transplantation, cells were collected from the spleen and subjected to flow cytometry. hCD45-positive percentages were calculated. Similar results were obtained at 6 and 12 weeks after transplantation (data not shown). The error bars represent average ± SD (n = 3).

(C and D) Various hematopoietin expression was examined by RT-PCR in immature hESCs (ihESCs), hESCdBAs, and hMSCdWAs (C). Hematopoietin expression in hESCdBAs after isoproterenol treatments was examined over time by RT-PCR (D).

(E and F) 5-FU treatment assay. Experimental procedure (E) and the results of BM-enucleated cell counts (F) were shown. The error bars represent average ± SD (n = 3).

hESC/hiPSC-derived spheres were further cultured on gelatin-coated 6-well plates using the above-described serum-free medium supplemented with the hematopoietic cytokine cocktail II (5 ng/ml IGF-II, 10 ng/ml BMP7, 5 ng/ml VEGFA, 20 ng/ml KITLG, 2.5 ng/ml FLT3LG, 2.5 ng/ml IL-6) for several days.

Protein Expression Analyses

Immunostaining was performed using a goat polyclonal anti-human UCP1 antibody (sc-6528, Santa Cruz Biotechnology, Inc.) or a rabbit polyclonal anti-human SOD2 antibody LS-C39331, LifeSpan BioSciences Inc., Seattle, WA) as described previously (Nakahara et al., 2009). Western blotting was performed using a rabbit polyclonal UCP1 (Ab10983) (Abcam plc., Cambridge, UK) as described previously (Nakahara et al., 2009).

Gene Expression Analyses

RT-PCR was performed using primers described in Supplemental Information. Quantitative RT-PCR (qPCR) was performed by applying SYBR Green qPCR method using primers purchased from SuperArray (QIAGEN Science, Maryland, USA) as described in the Supplemental Experimental Procedures. The results were normalized by *GAPDH*.

Electron Microscopic Examinations

Cells were fixed by 2.5% glutaraldehyde. Postfixation by 2% osmium tetroxide, along with sample embedding into resin and slicing, was performed by Bio Medical Laboratories Co. Ltd. (Tokyo, Japan) (Saeki et al., 2000).

Inhibitor Analyses

BA differentiation was performed by adding the following inhibitors to the differentiation medium: 10 μM p38 MAP kinase inhibitor (Cat 506126) (Calbiochem Co., Darmstadt, Germany), 50 μM MEK1 inhibitor (PD 98059) (Calbiochem Co.), 10 μM BMPR1a inhibitor (Dorsomorphin Dihydrochloride, Cat 047-31801) (WAKO Pure Chemical Industries, Osaka, Japan), and 10 μM Akt inhibitor IV (Cat 124011) (Calbiochem Co.).

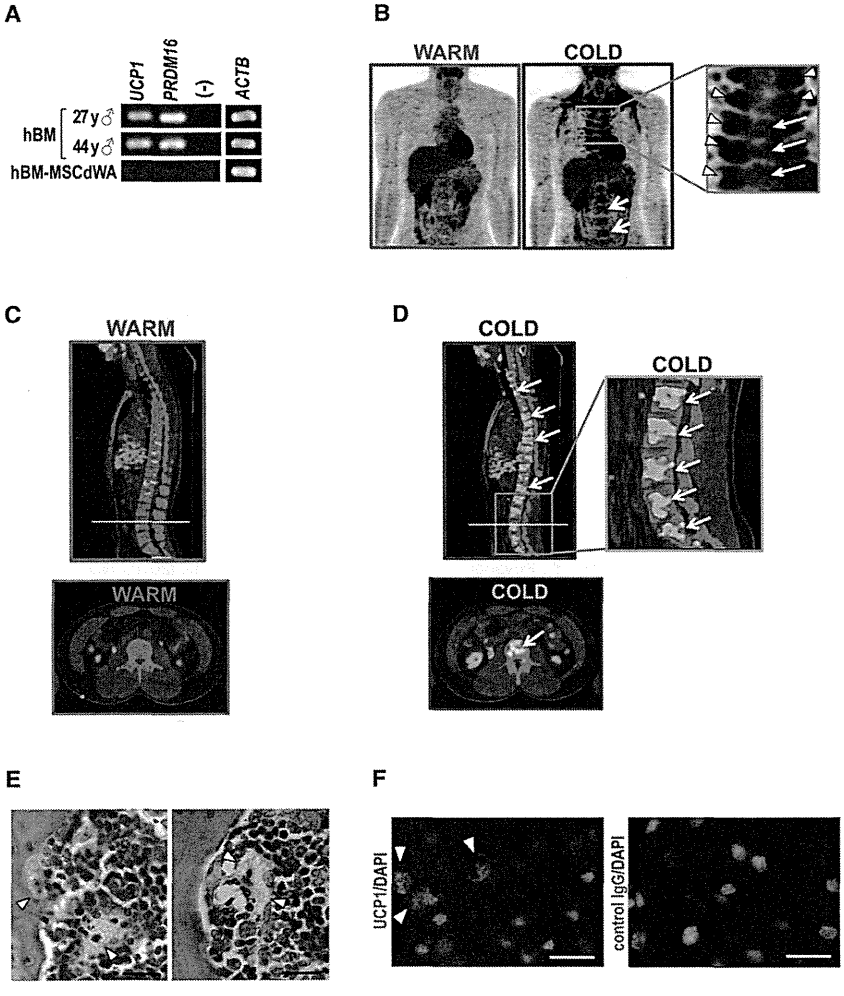

Figure 7. Examinations on BM-BAT

(A) Expression of *PRDM16* and *UCP1* in BM RNA samples of 27-year-old and 41-year-old males and human BM-derived hMSCdWA (hBM-MCdWA).

(B) ^{18}F-FDG-PET/CT. Typical results of the frontal images under warm and cold conditions were shown. Arrows indicate ^{18}F-FDG uptake into vertebrae per se, and arrowheads indicate ^{18}F-FDG uptake into classical paravertebral BA.

(C and D) Shown are sagittal and axial section images of ^{18}F-FDG-PET/CT under warm (C) and cold conditions (D). Arrows indicate the ^{18}F-FDG uptake into vertebral BM.

(E and F) Thoracic vertebra of 3-week-old ICR mice was subjected to HE staining (E) or UCP1 immunostaining (FF). Arrowheads indicate the existence of BA.

were measured by Accutrend Plus (F. Hoffmann-La Roche, Ltd., Basel, Switzerland). For oral fat tolerance tests, ICR mice were subcutaneously transplanted with immature hPSC or hPSCdBA and kept abstained from feed. After 16 hr, isoproterenol (15 μmol/kg) was administrated. After another 2 hr, 200 μl of olive oil was orally administrated, and blood TG levels were measured every 2 hr.

Assessment of Glucose Metabolism

The 1 × 10^6 of hESCdBA or hMSCdWA was transplanted to 6- or 10-week-old male ICR mice, which were kept abstained from feed. After 16 hr, isoproterenol (30 μmol/kg) was administrated. After another 4 hr, 2 g/kg of glucose (041-00595, Wako Pure Chemical Industries, Ltd., Osaka, Japan) was orally administrated. Blood sample were taken after 0, 15, 30, and 60 min. Blood glucose concentrations were measured by Accutrend Plus, and plasma insulin concentrations were measured by mouse insulin ELISA kit (Morinaga Institute of Biological Science, Inc., Yokohama, Japan).

Oxygen Consumption Analyses

The adherent culture step of BA differentiation was performed on special 96-well plates (Seahorse Bioscience Inc., Billerica, MA) precoated by 0.1% gelatin by seeding 30 spheres per well. Oxygen consumption was analyzed by Extracellular Flux Analyzer XF96 (Seahorse Bioscience Inc.) according to the manufacturer's guidance.

Calorigenic Analyses

The 1 × 10^6 of hPSCdBA or immature hPSCs were suspended in 100 μl saline and subcutaneously transplanted into 5-week-old male ICR mice After 24 hr, 30 μmol/kg of isoproterenol (12760, Sigma Chemical Co.) was administrated from the tail vein. After another 4 hr, mice were anesthetized, and dermal temperature was measured by Thermo GEAR G120/G100 (NEC Avio Infrared Technologies Co., Ltd, Tokyo, Japan). All animal care procedures involved in calorigenic analyses, assessment of lipid and metabolism, and hematopoietic stromal assays were approved by the Animal Care and Use Committee of the Research Institute, National Center for Global Health and Medicine (NCGM), and complied with the procedures of the Guide for the Care and Use of Laboratory Animals of NCGM.

Assessment of Lipid Metabolism

Six-week-old male CR mice were subcutaneously transplanted with 1 × 10^6 of immature hESC, hESCdBA, or hMC-derived WA suspended in 100 μl saline and kept abstained from feed. After 16 hr, isoproterenol (30 μmol/kg) was administrated. After another 2 hr, blood samples were taken, and TG concentrations

Hematopoietic Stromal Assays

The human cord blood CD34$^+$ cells were cultured on hPSCdBA layers without recombinant cytokines in RPMI1640 medium supplemented with 10% fetal calf serum. Floating cells were collected after 7 days, and 2 × 10^5 cells were transplanted into tibial bone marrow of NOG mice. After 6, 8, and 12 weeks, cells were collected from contralateral femoral bone marrow and spleen and subjected to cytometry using an anti-human CD45-FITC (clone J33) (Beckman Coulter Inc.) and anti-human CD33-PE antibody (clone WM53) (BD Biosciences, San Jose, CA). For control, cord blood CD34$^+$ cells were directly transplanted without coculture. For myelosuppression recovery assays, 100 mg/kg of 5-FU was intraperitoneally administrated. From day 3 to day 6, 30 μmol/kg of isoproterenol was administrated from tail vein. At day 7, bone marrow cells were collected from femoral bones and analyzed.

^{18}F-FDG-PET/CT Examinations

After careful instruction regarding the study and informed consent to participants, PET/CT examinations of healthy young volunteers (24.8 ± 5.8 years of age, n = 20) were performed. The protocol was approved by the institutional review boards of Tenshi College. Standardized uptake value (SUV) was measured by an expert as described in the Supplemental Experimental Procedures. Data are reported as means ± SEM. Statistics analyses were performed using SPSS software, version 18 (International Business Machines

Corp, New York), as described in the Supplemental Experimental Procedures. P values are considered to be statistically significant if <0.05.

SUPPLEMENTAL INFORMATION

Supplemental Information includes seven figures, Supplemental Experimental Procedures, and Supplemental References and can be found with this article online at http://dx.doi.org/10.1016/j.cmet.2012.08.001.

ACKNOWLEDGMENTS

This work was supported by Grant-in-Aid from Ministry of Health, Labour and Welfare of Japan (KHD1017) and by Japan Science and Technology Agency (AS 2321379G). We thank Mr. Kameya at LSI Sapporo Clinic for technical assistance for PET-CT examinations and Mr. Obara at LSI Sapporo Clinic for general assistance.

Received: March 17, 2012
Revised: June 30, 2012
Accepted: August 1, 2012
Published online: September 4, 2012

REFERENCES

Ahfeldt, T., Schinzel, R.T., Lee, Y.K., Hendrickson, D., Kaplan, A., Lum, D.H., Camahort, R., Xia, F., Shay, J., Rhee, E.P., et al. (2012). Programming human pluripotent stem cells into white and brown adipocytes. Nat. Cell Biol. *14*, 209–219.

Arai, F., and Suda, T. (2007). Maintenance of quiescent hematopoietic stem cells in the osteoblastic niche. Ann. N Y Acad. Sci. *1106*, 41–53.

Asano, A., Morimatsu, M., Nikami, H., Yoshida, T., and Saito, M. (1997). Adrenergic activation of vascular endothelial growth factor mRNA expression in rat brown adipose tissue: implication in cold-induced angiogenesis. Biochem. J. *328*, 179–183.

Bartelt, A., Bruns, O.T., Reimer, R., Hohenberg, H., Ittrich, H., Peldschus, K., Kaul, M.G., Tromsdorf, U.I., Weller, H., Waurisch, C., et al. (2011). Brown adipose tissue activity controls triglyceride clearance. Nat. Med. *17*, 200–205.

Braun, T., and Arnold, H.H. (1996). Myf-5 and myoD genes are activated in distinct mesenchymal stem cells and determine different skeletal muscle cell lineages. EMBO J. *15*, 310–318.

Calo, E., Quintero-Estades, J.A., Danielian, P.S., Nedelcu, S., Berman, S.D., and Lees, J.A. (2010). Rb regulates fate choice and lineage commitment in vivo. Nature *466*, 1110–1114.

Cossu, G., Kelly, R., Tajbakhsh, S., Di Donna, S., Vivarelli, E., and Buckingham, M. (1996). Activation of different myogenic pathways: myf-5 is induced by the neural tube and MyoD by the dorsal ectoderm in mouse paraxial mesoderm. Development *122*, 429–437.

Crisan, M., Yap, S., Casteilla, L., Chen, C.W., Corselli, M., Park, T.S., Andriolo, G., Sun, B., Zheng, B., Zhang, L., et al. (2008). A perivascular origin for mesenchymal stem cells in multiple human organs. Cell Stem Cell *3*, 301–313.

Cypess, A.M., Lehman, S., Williams, G., Tal, I., Rodman, D., Goldfine, A.B., Kuo, F.C., Palmer, E.L., Tseng, Y.H., Doria, A., et al. (2009). Identification and importance of brown adipose tissue in adult humans. N. Engl. J. Med. *360*, 1509–1517.

Dexter, T.M., Allen, T.D., and Lajtha, L.G. (1977). Conditions controlling the proliferation of haemopoietic stem cells in vitro. J. Cell. Physiol. *91*, 335–344.

Elabd, C., Chiellini, C., Carmona, M., Galitzky, J., Cochet, O., Petersen, R., Pénicaud, L., Kristiansen, K., Bouloumié, A., Casteilla, L., et al. (2009). Human multipotent adipose-derived stem cells differentiate into functional brown adipocytes. Stem Cells *27*, 2753–2760.

Enerbäck, S., Jacobsson, A., Simpson, E.M., Guerra, C., Yamashita, H., Harper, M.E., and Kozak, L.P. (1997). Mice lacking mitochondrial uncoupling protein are cold-sensitive but not obese. Nature *387*, 90–94.

Feldmann, H.M., Golozoubova, V., Cannon, B., and Nedergaard, J. (2009). UCP1 ablation induces obesity and abolishes diet-induced thermogenesis in mice exempt from thermal stress by living at thermoneutrality. Cell Metab. *9*, 203–209.

Gimble, J.M., Dorheim, M.A., Cheng, Q., Medina, K., Wang, C.S., Jones, R., Koren, E., Pietrangeli, C., and Kincade, P.W. (1990). Adipogenesis in a murine bone marrow stromal cell line capable of supporting B lineage lymphocyte growth and proliferation: biochemical and molecular characterization. Eur. J. Immunol. *20*, 379–387.

Gimble, J.M., Youkhana, K., Hua, X., Bass, H., Medina, K., Sullivan, M., Greenberger, J., and Wang, C.S. (1992). Adipogenesis in a myeloid supporting bone marrow stromal cell line. J. Cell. Biochem. *50*, 73–82.

Gupta, R.K., Mepani, R.J., Kleiner, S., Lo, J.C., Khandekar, M.J., Cohen, P., Frontini, A., Bhowmick, D.C., Ye, L., Cinti, S., et al. (2012). Zfp423 expression identifies committed preadipocytes and localizes to adipose endothelial and perivascular cells. Cell Metab. *15*, 230–239.

Hiroyama, T., Miharada, K., Aoki, N., Fujioka, T., Sudo, K., Danjo, I., Nagasawa, T., and Nakamura, Y. (2006). Long-lasting in vitro hematopoiesis derived from primate embryonic stem cells. Exp. Hematol. *34*, 760–769.

Hofer, M., Pospísil, M., Znojil, V., Holá, J., Vacek, A., and Streitová, D. (2007). Adenosine A(3) receptor agonist acts as a homeostatic regulator of bone marrow hematopoiesis. Biomed. Pharmacother. *61*, 356–359.

Ito, M., Hiramatsu, H., Kobayashi, K., Suzue, K., Kawahata, M., Hioki, K., Ueyama, Y., Koyanagi, Y., Sugamura, K., Tsuji, K., et al. (2002). NOD/SCID/gamma(c)(null) mouse: an excellent recipient mouse model for engraftment of human cells. Blood *100*, 3175–3182.

Jacene, H.A., Cohade, C.C., Zhang, Z., and Wahl, R.L. (2011). The relationship between patients' serum glucose levels and metabolically active brown adipose tissue detected by PET/CT. Mol. Imaging Biol. *13*, 1278–1283.

Jackson, D.M., Hambly, C., Trayhurn, P., and Speakman, J.R. (2001). Can non-shivering thermogenesis in brown adipose tissue following NA injection be quantified by changes in overlying surface temperatures using infrared thermography? J. Therm. Biol. *26*, 85–93.

Kiel, M.J., and Morrison, S.J. (2006). Maintaining hematopoietic stem cells in the vascular niche. Immunity *25*, 862–864.

Kontani, Y., Wang, Y., Kimura, K., Inokuma, K.I., Saito, M., Suzuki-Miura, T., Wang, Z., Sato, Y., Mori, N., and Yamashita, H. (2005). UCP1 deficiency increases susceptibility to diet-induced obesity with age. Aging Cell *4*, 147–155.

Krings, A., Rahman, S., Huang, S., Lu, Y., Czernik, P.J., and Lecka-Czernik, B. (2012). Bone marrow fat has brown adipose tissue characteristics, which are attenuated with aging and diabetes. Bone *50*, 546–552.

Laharrague, P., Fontanilles, A.M., Tkaczuk, J., Corberand, J.X., Pénicaud, L., and Casteilla, L. (2000). Inflammatory/haematopoietic cytokine production by human bone marrow adipocytes. Eur. Cytokine Netw. *11*, 634–639.

Motyl, K.J., and Rosen, C.J. (2011). Temperatures rising: brown fat and bone. Discov. Med. *11*, 179–185.

Nagasawa, T. (2007). The chemokine CXCL12 and regulation of HSC and B lymphocyte development in the bone marrow niche. Adv. Exp. Med. Biol. *602*, 69–75.

Nakahara, M., Nakamura, N., Matsuyama, S., Yogiashi, Y., Yasuda, K., Kondo, Y., Yuo, A., and Saeki, K. (2009). High-efficiency production of subculturable vascular endothelial cells from feeder-free human embryonic stem cells without cell-sorting technique. Cloning Stem Cells *11*, 509–522.

Naveiras, O., Nardi, V., Wenzel, P.L., Hauschka, P.V., Fahey, F., and Daley, G.Q. (2009). Bone-marrow adipocytes as negative regulators of the haematopoietic microenvironment. Nature *460*, 259–263.

Ookura, N., Fujimori, Y., Nishioka, K., Kai, S., Hara, H., and Ogawa, H. (2007). Adipocyte differentiation of human marrow mesenchymal stem cells reduces the supporting capacity for hematopoietic progenitors but not for severe combined immunodeficiency repopulating cells. Int. J. Mol. Med. *19*, 387–392.

Osafune, K., Caron, L., Borowiak, M., Martinez, R.J., Fitz-Gerald, C.S., Sato, Y., Cowan, C.A., Chien, K.R., and Melton, D.A. (2008). Marked differences in differentiation propensity among human embryonic stem cell lines. Nat. Biotechnol. *26*, 313–315.

Ouellet, V., Routhier-Labadie, A., Bellemare, W., Lakhal-Chaieb, L., Turcotte, E., Carpentier, A.C., and Richard, D. (2011). Outdoor temperature, age, sex, body mass index, and diabetic status determine the prevalence, mass, and glucose-uptake activity of 18F-FDG-detected BAT in humans. J. Clin. Endocrinol. Metab. *96*, 192–199.

Petrovic, N., Walden, T.B., Shabalina, I.G., Timmons, J.A., Cannon, B., and Nedergaard, J. (2010). Chronic peroxisome proliferator-activated receptor gamma (PPARgamma) activation of epididymally derived white adipocyte cultures reveals a population of thermogenically competent, UCP1-containing adipocytes molecularly distinct from classic brown adipocytes. J. Biol. Chem. *285*, 7153–7164.

Reznikoff, C.A., Brankow, D.W., and Heidelberger, C. (1973). Establishment and characterization of a cloned line of C3H mouse embryo cells sensitive to postconfluence inhibition of division. Cancer Res. *33*, 3231–3238.

Saeki, K., Yuo, A., Okuma, E., Yazaki, Y., Susin, S.A., Kroemer, G., and Takaku, F. (2000). Bcl-2 down-regulation causes autophagy in a caspase-independent manner in human leukemic HL60 cells. Cell Death Differ. *7*, 1263–1269.

Saito, M., Okamatsu-Ogura, Y., Matsushita, M., Watanabe, K., Yoneshiro, T., Nio-Kobayashi, J., Iwanaga, T., Miyagawa, M., Kameya, T., Nakada, K., et al. (2009). High incidence of metabolically active brown adipose tissue in healthy adult humans: effects of cold exposure and adiposity. Diabetes *58*, 1526–1531.

Sakurai, H., Era, T., Jakt, L.M., Okada, M., Nakai, S., Nishikawa, S., and Nishikawa, S. (2006). In vitro modeling of paraxial and lateral mesoderm differentiation reveals early reversibility. Stem Cells *24*, 575–586.

Seale, P., Kajimura, S., Yang, W., Chin, S., Rohas, L.M., Uldry, M., Tavernier, G., Langin, D., and Spiegelman, B.M. (2007). Transcriptional control of brown fat determination by PRDM16. Cell Metab. *6*, 38–54.

Seale, P., Bjork, B., Yang, W., Kajimura, S., Chin, S., Kuang, S., Scimè, A., Devarakonda, S., Conroe, H.M., Erdjument-Bromage, H., et al. (2008). PRDM16 controls a brown fat/skeletal muscle switch. Nature *454*, 961–967.

Sellayah, D., Bharaj, P., and Sikder, D. (2011). Orexin is required for brown adipose tissue development, differentiation, and function. Cell Metab. *14*, 478–490.

Suemori, H., Yasuchika, K., Hasegawa, K., Fujioka, T., Tsuneyoshi, N., and Nakatsuji, N. (2006). Efficient establishment of human embryonic stem cell lines and long-term maintenance with stable karyotype by enzymatic bulk passage. Biochem. Biophys. Res. Commun. *345*, 926–932.

Sun, L., Xie, H., Mori, M.A., Alexander, R., Yuan, B., Hattangadi, S.M., Liu, Q., Kahn, C.R., and Lodish, H.F. (2011). Mir193b-365 is essential for brown fat differentiation. Nat. Cell Biol. *13*, 958–965.

Takayama, N., Nishikii, H., Usui, J., Tsukui, H., Sawaguchi, A., Hiroyama, T., Eto, K., and Nakauchi, H. (2008). Generation of functional platelets from human embryonic stem cells in vitro via ES-sacs, VEGF-promoted structures that concentrate hematopoietic progenitors. Blood *111*, 5298–5306.

Tanaka, Y., and Inoue, T. (1976). Fatty marrow in the vertebrae. A parameter for hematopoietic activity in the aged. J. Gerontol. *31*, 527–532.

Thorns, C., Schardt, C., Katenkamp, D., Kähler, C., Merz, H., and Feller, A.C. (2008). Hibernoma-like brown fat in the bone marrow: report of a unique case. Virchows Arch. *452*, 343–345.

Timmons, J.A., Wennmalm, K., Larsson, O., Walden, T.B., Lassmann, T., Petrovic, N., Hamilton, D.L., Gimeno, R.E., Wahlestedt, C., Baar, K., et al. (2007). Myogenic gene expression signature establishes that brown and white adipocytes originate from distinct cell lineages. Proc. Natl. Acad. Sci. USA *104*, 4401–4406.

Tonello, C., Giordano, A., Cozzi, V., Cinti, S., Stock, M.J., Carruba, M.O., and Nisoli, E. (1999). Role of sympathetic activity in controlling the expression of vascular endothelial growth factor in brown fat cells of lean and genetically obese rats. FEBS Lett. *442*, 167–172.

Tran, K.V., Gealekman, O., Frontini, A., Zingaretti, M.C., Morroni, M., Giordano, A., Smorlesi, A., Perugini, J., De Matteis, R., Sbarbati, A., et al. (2012). The vascular endothelium of the adipose tissue gives rise to both white and brown fat cells. Cell Metab. *15*, 222–229.

Tseng, Y.H., Kokkotou, E., Schulz, T.J., Huang, T.L., Winnay, J.N., Taniguchi, C.M., Tran, T.T., Suzuki, R., Espinoza, D.O., Yamamoto, Y., et al. (2008). New role of bone morphogenetic protein 7 in brown adipogenesis and energy expenditure. Nature *454*, 1000–1004.

van Marken Lichtenbelt, W.D., Vanhommerig, J.W., Smulders, N.M., Drossaerts, J.M., Kemerink, G.J., Bouvy, N.D., Schrauwen, P., and Teule, G.J. (2009). Cold-activated brown adipose tissue in healthy men. N. Engl. J. Med. *360*, 1500–1508.

Virtanen, K.A., Lidell, M.E., Orava, J., Heglind, M., Westergren, R., Niemi, T., Taittonen, M., Laine, J., Savisto, N.J., Enerbäck, S., and Nuutila, P. (2009). Functional brown adipose tissue in healthy adults. N. Engl. J. Med. *360*, 1518–1525.

Yoneshiro, T., Aita, S., Matsushita, M., Okamatsu-Ogura, Y., Kameya, T., Kawai, Y., Miyagawa, M., Tsujisaki, M., and Saito, M. (2011). Age-related decrease in cold-activated brown adipose tissue and accumulation of body fat in healthy humans. Obesity (Silver Spring) *19*, 1755–1760.